

Hydrogen promotes the activation of Cu, Zn superoxide dismutase in a rat corneal alkali-burn model

Takeshi Arima^{1,2}, Tsutomu Igarashi¹, Masaaki Uchiyama¹, Maika Kobayashi¹, Ikuroh Ohsawa³, Akira Shimizu², Hiroshi Takahashi¹

¹Department of Ophthalmology, Nippon Medical School, Tokyo 113-8602, Japan

²Department of Analytic Human Pathology, Nippon Medical School, Tokyo 113-8602, Japan

³Biological Process of Aging, Tokyo Metropolitan Institute of Gerontology, Tokyo 173-0015, Japan

Correspondence to: Takeshi Arima. Department of Ophthalmology, Nippon Medical School, 1-1-5, Sendagi, Bunkyo-ku, Tokyo 113-8602, Japan. takesuii0714@nms.ac.jp

Received: 2019-09-26 Accepted: 2020-05-12

Abstract

• **AIM:** To investigate the effects of hydrogen (H₂) on Cu, Zn superoxide dismutase (SOD1) activation in a rat model of corneal alkali burn.

• **METHODS:** In each rat, one cornea was subjected to alkali exposure. Physiological saline (saline group) or H₂-dissolved saline (H₂ group) was instilled continuously on the cornea for 5min before and after alkali exposure. Inflammatory cells, neovascularization, and cytoplasmic SOD1 levels were evaluated immunohistochemically in enucleated eyes from both groups. Three-dimensional ultrastructural tissue changes in the eyes were analyzed using low-vacuum scanning electron microscopy.

• **RESULTS:** The numbers of both inflammatory and vascular endothelial cells were significantly reduced in the corneas of the H₂ group ($P<0.01$). Furthermore, H₂ treatment increased both cytoplasmic SOD1 levels ($P<0.01$) and activity in corneal epithelial cells ($P<0.01$). Notably, the SOD1 activity level in the H₂ group was approximately 2.5-fold greater than that in the saline group.

• **CONCLUSION:** H₂ treatment suppresses inflammation and neovascularization in the injured cornea and indirectly suppresses oxidative insult to the cornea by upregulating the SOD1 enzyme protein level and activity.

• **KEYWORDS:** hydrogen; alkali burn; Cu, Zn superoxide dismutase; low-vacuum scanning electron microscopy; rats

DOI:10.18240/ijo.2020.08.01

Citation: Arima T, Igarashi T, Uchiyama M, Kobayashi M, Ohsawa I, Shimizu A, Takahashi H. Hydrogen promotes the activation of Cu, Zn superoxide dismutase in a rat corneal alkali-burn model. *Int J Ophthalmol* 2020;13(8):1173-1179

INTRODUCTION

Since we initially proposed a role for hydrogen (H₂) as a therapeutic antioxidant *via* the selective reduction of cytotoxic oxygen radicals in 2007^[1], several studies have demonstrated the usefulness of H₂ and suggested its potential in therapeutic applications^[2]. Accordingly, the field of H₂ medicine is rapidly growing, and more than 25 clinical studies (including double-blind clinical trials) are currently evaluating the therapeutic effectiveness of H₂^[3-4]. More specifically, ophthalmology researchers have reported the applications of H₂ to directly reduce oxidative stress in the contexts of retinal artery occlusion^[5], corneal alkali burn^[6], and phacoemulsification cataract surgery^[7]. Notably, however, H₂ has also been reported to suppress oxidative stress indirectly *via* other pathways^[8-12].

Activation of the cytoplasmic Cu, Zn superoxide dismutase (SOD1) enzyme, which is involved in antioxidant stress, is one pathway identified in studies of H₂ medicine^[13]. SOD1 regulates reactive oxygen species levels, thus playing an important role in tissue homeostasis. Reports have demonstrated the involvement of H₂ in SOD1 activity and suggested that the former indirectly suppressed antioxidant stress^[2,9]. To date, however, few reports have described the effects of H₂ in the activation of SOD1 in an ophthalmological context.

Therefore, in the current study, we evaluated the effects of H₂ on inflammation and neovascularization, as well as the indirect effects on oxidative stress, by clarifying the influences of H₂ on SOD1 activity in the corneal alkali burn model.

MATERIALS AND METHODS

Ethical Approval All animal-based experiments were conducted in compliance with the Experimental Animal Ethics Review Committee of Nippon Medical School (No.29-055). All procedures conformed with the guidelines of the Association for Research in Vision and Ophthalmic and Visual Research.

Animals Eight-week-old male Wistar rats weighing 200 g were obtained from Sankyo Laboratory Service (Tokyo, Japan). Rats were housed in a specific pathogen free environment with a 12h light/12h dark cycle. Water and food were available and continuous clinical care (24h per day/7d per week) was provided throughout the experiment to ensure prompt intervention when needed.

Methods

Alkali burn model and preparation of H₂-dissolved saline

One eye of each rat ($n=104$ in total) was subjected to an alkali burn under 3.5% isoflurane inhalation anesthesia, according to the following protocol: a circular piece of filter paper (diameter: 3.2 mm) soaked in 1 mol/L NaOH was placed on the central cornea for 1min. The corneas were rinsed *via* dripping (10 mL/min) with physiologic saline (saline group: $n=39$) or H₂-dissolved saline (H₂ group: $n=39$) for 5min prior to alkali exposure, and again after alkali exposure. In each rat, the uninjured normal cornea was used as a control.

H₂-dissolved saline was prepared as described in our previous report^[7]. Briefly, commercially available saline plastic bags (Otsuka Pharmaceutical, Tokyo, Japan) were placed in an acrylic vacuum chamber filled with H₂ gas for 24h (Figure 1A). Prior to use, the dissolved concentration of H₂ in each bag was confirmed using a needle-type H₂ sensor (Unisense, Aarhus, Denmark). In all experiments, H₂-dissolved saline was used within 5min after retrieval from the vacuum chamber.

Rats were euthanized by exsanguination under 3.5% isoflurane inhalation anesthesia at 6h, 1, and 7d after alkali injury. The enucleated eyes were subjected to histological and immunohistochemical examination and low-vacuum scanning electron microscopy (LV-SEM). No adverse events were noted throughout the experiment.

Histological and immunohistochemical analysis and LV-SEM observation

The enucleated eyes ($n=8$ for each group/for each endpoint) were fixed in 10% buffered formalin and embedded in paraffin prior to light microscopic observation. Subsequently, deparaffinized tissue sections (thickness: 2.5 μ m) were stained with hematoxylin and eosin (HE), Naphtol AS-D chloroacetate esterase (EST) to detect infiltrating neutrophils^[14], and LV-SEM. For the latter, tissues were stained with periodic acid-methenamine silver (PAM) to specify collagens^[15-16].

For the immunohistochemical analysis of inflammatory cells, neovascularization, and SOD1 enzyme levels, the number of positive cells per sample was measured pathologically in high-power fields (magnification: 400 \times) located in two corneal areas (center: 3 fields, periphery: 2 fields). The following primary antibodies were used: 1) monoclonal mouse anti-aminopeptidase P antibody (JG12; Thermo Scientific, Rockford, IL, USA) to detect vascular endothelial cells^[17], 2)

monoclonal mouse anti-8-OHdG antibody (JaICA, Shizuoka, Japan) to detect DNA oxidative stress^[18], 3) monoclonal mouse anti-CD68 antibody (ED1; BMA, Nagoya, Japan) to detect pan-macrophages, 4) monoclonal mouse anti-CD163 antibody (ED2; BMA, Nagoya, Japan) to detect M2 macrophages, and 5) polyclonal rabbit anti-SOD1 antibody (Stressgen, Victoria, BC, Canada) to detect SOD1 enzyme. As noted above, samples for LV-SEM were subjected to PAM staining for contrast enhancement. After staining with PAM, specimens lacking a mounting cover glass were examined *via* LV-SEM (Hitachi Tabletop Microscope TM3030, Hitachi High-Technologies Corp., Tokyo, Japan)^[19-20]. Ultrastructural alterations in the corneal wound were assessed using an acceleration voltage of 15 kV under 30 Pa for the backscattered electron detector.

Statistical Analyses All results are expressed as means \pm standard deviations (SD). The statistical analysis was performed using an analytical software program (Excel; Microsoft, Redmond, WA, USA). Student's *t*-test was used to evaluate comparisons. The results were considered statistically significant when $P<0.05$.

RESULTS

H₂ Concentration in the Solution After a 24-hour exposure to 100% H₂ gas in an acrylic vacuum chamber (Figure 1A), the saline bag contained a dissolved H₂ concentration of 87.2%. In other words, the H₂ gas easily penetrated the plastic bag, and the solution was nearly equilibrated with the ambient H₂ gas within 24h. After retrieval from the chamber, however, the H₂ concentration in the bag decreased to 61.2% over 30min (Figure 1B). Initially, the H₂ concentration at the exit of infusion tube was 53.8% under continuous irrigation (10 mL/min) but decreased to 47.2% in 30min (Figure 1B).

Effects of H₂ on Tissue Damage HE staining revealed various inflammatory cells in the corneal limbus on day 1. Although these cells visibly infiltrated the center of the cornea on day 7 in the saline group, such changes were remarkably minimal in the H₂ group (Figure 2A). Similarly, anterior segment photography showed severe hyphema and corneal opacity in the saline group on day 7, with minimal changes in the H₂ group (Figure 2B).

Effects of H₂ on Corneal Neovascularization Vascular endothelial cell-specific JG12 staining was used to evaluate neovascularization (Figure 3A). Specifically, the degree of neovascularization was assessed by counting the labeled capillary lumens in a microscopic field. In the H₂ group, neovascularization was suppressed by approximately 60% on day 7 relative to the saline group (Figure 3B).

Effects of H₂ on Inflammatory Cells Figure 4A depicts EST-positive neutrophils in the limbus at 6h and in the central cornea on day 1 and 8-OHdG-positive cells in the central cornea on day 1. Here, EST-positive neutrophils infiltrated the

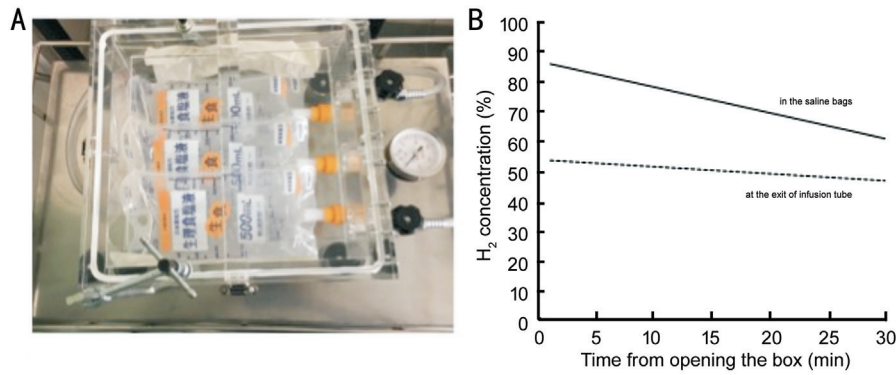


Figure 1 Preparation of H₂-dissolved saline and measurement of H₂ concentration A: Saline bags were placed in an acrylic vacuum chamber in which the air was replaced with 100% H₂ gas; B: H₂ concentrations in the saline bags and at the exit of the infusion tube within 30min. The full line indicates the H₂ concentration in the saline bags and the broken line indicates the H₂ concentration at the exit of the infusion tube.

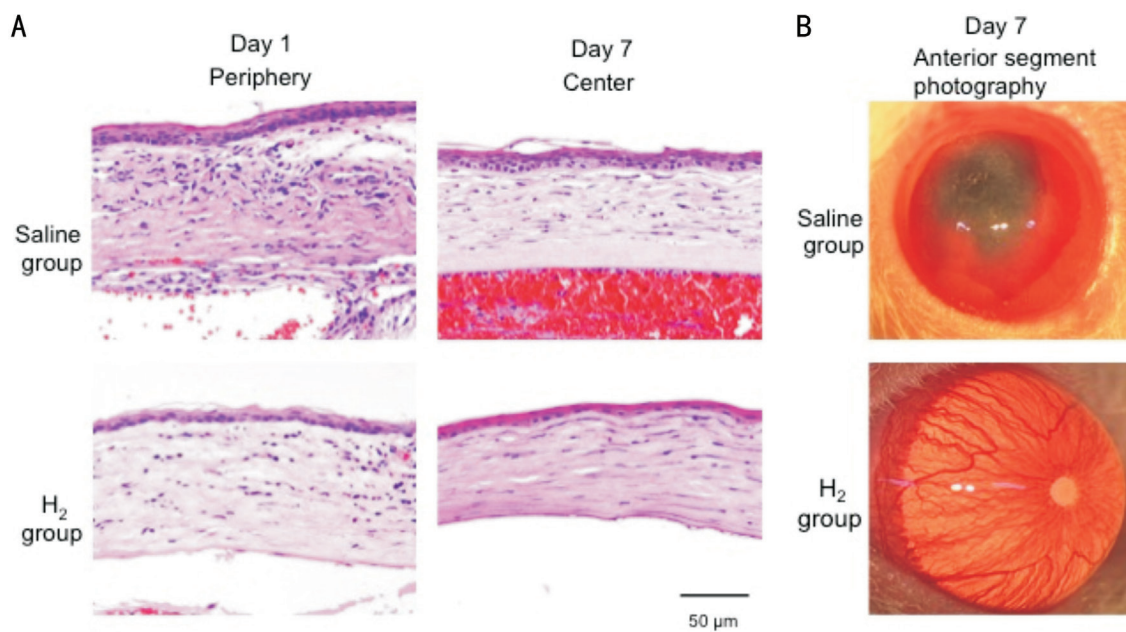


Figure 2 Effects of H₂ instillation on rat corneal alkali injuries A: The histological effects of H₂ treatment were investigated in HE-stained corneal sections; B: A comparison of anterior segment photography of eyes from the H₂ and saline groups on day 7. *n*=20/104 in total, *n*=5 for each group/for each endpoint.

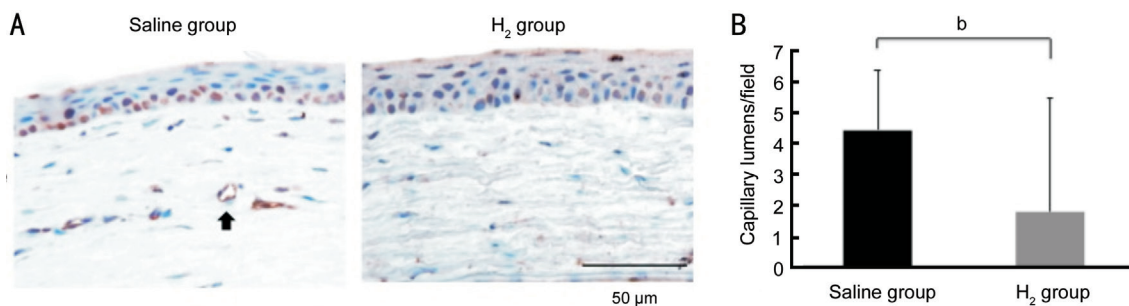


Figure 3 Evaluation of corneal neovascularization in response to H₂ treatment A: Immunohistochemical evaluation of JG12-positive vascular endothelial cells (arrow) in the corneal center on day 7; B: The capillary lumens in the corneal center were significantly reduced by H₂ treatment. *n*=48/104 in total, *n*=8 for each group/for each endpoint. ^b*P*<0.01.

area immediately proximal to the 8-OHdG-positive corneal stromal cells, suggesting the involvement of free radicals. At both time points, significantly smaller numbers of neutrophils were observed in the H₂ group, compared to the saline group

(Figure 4B). Furthermore, LV-SEM revealed structural changes in the stromal collagen fibers, as well as a smaller number of inflammatory cells within these fibers in the H₂ group, compared to the saline group (Figure 4C).

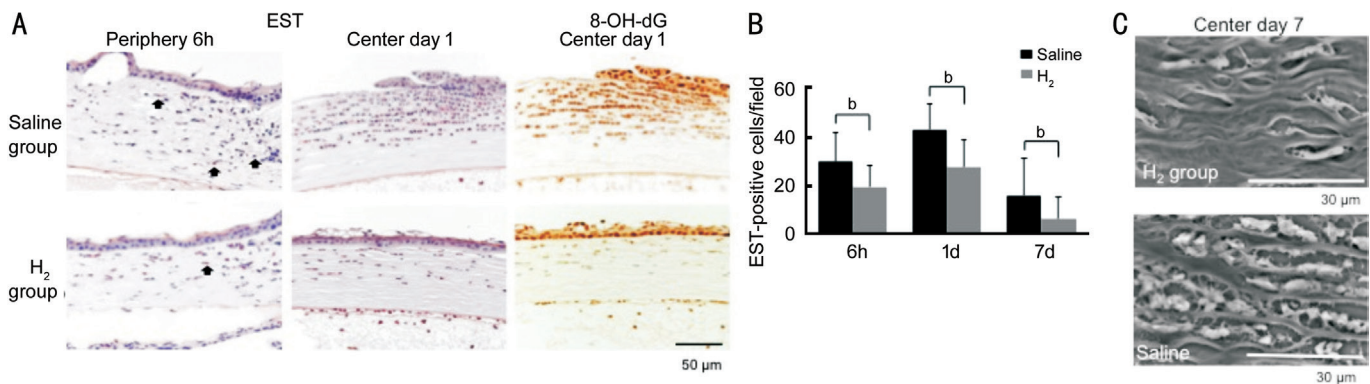


Figure 4 Effects of H₂ treatment on free radicals and neutrophil infiltration A: Representative images of EST-stained (arrow) injured corneas treated with saline or H₂ at each time point. Comparison of the association of EST-positive and 8-OH-dG-positive cells in an analysis of immunostained serial sections was also showed. B: Bar chart of the numbers of EST-positive cells in the peripheral cornea; a statistically significant difference between the H₂ and saline groups is apparent. C: Comparison of collagen fibers and infiltrating cells in both groups, using low-vacuum scanning electron microscopy and PAM staining. *n*=48/104 in total, *n*=8 for each group/for each endpoint. ^b*P*<0.01.

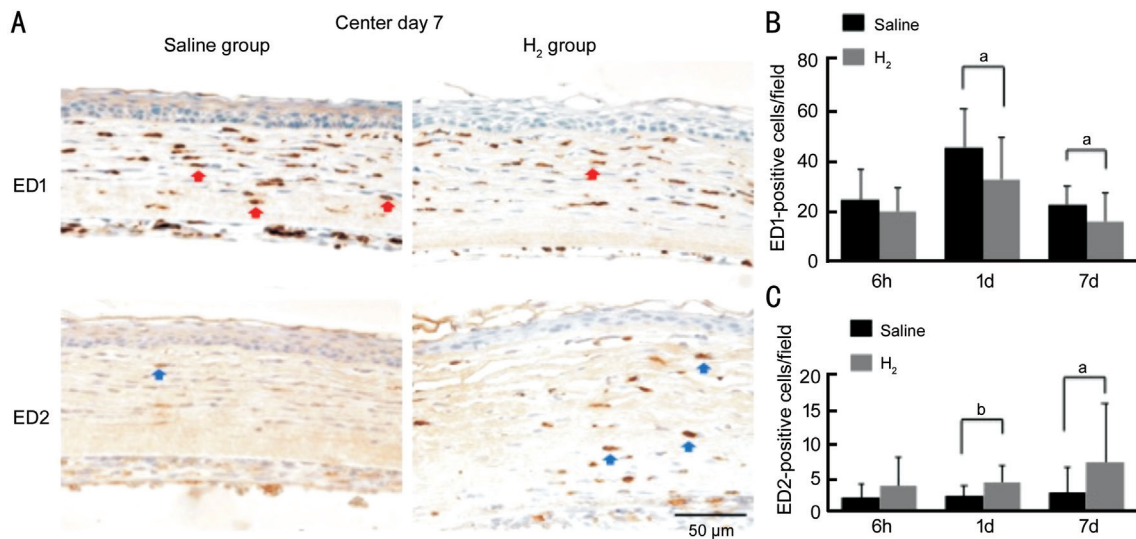


Figure 5 Phenotypic evaluation of macrophages in H₂ and saline-treated corneas A: Representative images of ED1 (red arrow) and ED2 (blue arrow) immunostained central corneal tissues from both groups. B: Bar chart of the numbers of ED1-positive macrophages in the peripheral corneas; H₂ therapy significantly reduced the number of ED1-positive macrophages. C: Bar chart of the numbers of ED2-positive macrophages in the peripheral corneas; a significant difference between the H₂ and saline groups was observed. *n*=48/104 in total, *n*=8 for each group/for each endpoint. ^a*P*<0.05, ^b*P*<0.01.

Additionally, ED1 and ED2 immunostaining were used to detect the infiltration of pan-macrophages and M2 macrophages, respectively (Figure 5A). Notably, H₂ significantly reduced the infiltration of ED1-positive pan-macrophages while significantly increasing that of ED2-positive M2 macrophages (Figure 5B and 5C).

Effects of H₂ on SOD1 enzyme activity To further explore the potential effects of H₂ on anti-oxidant enzymes, we investigated the protein levels of SOD1. Notably, the cytoplasmic SOD1 level in corneal epithelial cells was significantly greater in the H₂ group than in the saline group (Figure 6A). These SOD1 levels increased immediately after H₂ administration and then decreased over time (Figure 6B). At 6h post-injury, SOD1 expression in the central cornea

increased by approximately 4.8-fold in the H₂ group relative to the uninjured control, compared to 1.8-fold in the saline group (Figure 6C).

DISCUSSION

Strong inflammation and subsequent neovascularization are often observed in the alkali-burned cornea^[21-22]. Accordingly, the observed effects of H₂ have led to considerable interest in its application to alkali-induced corneal injury. Treatment with H₂ contributes to the protective effect against inflammatory injury by selectively reducing hydroxyl radical, the most cytotoxic of reactive oxygen species^[23-24]. Previously, Kubota *et al*^[6] evaluated the effect of H₂ in a mouse model involving an alkali burn in the SOD1-deficient cornea. Their findings proved the oxidative nature of the alkali burn injury and demonstrated

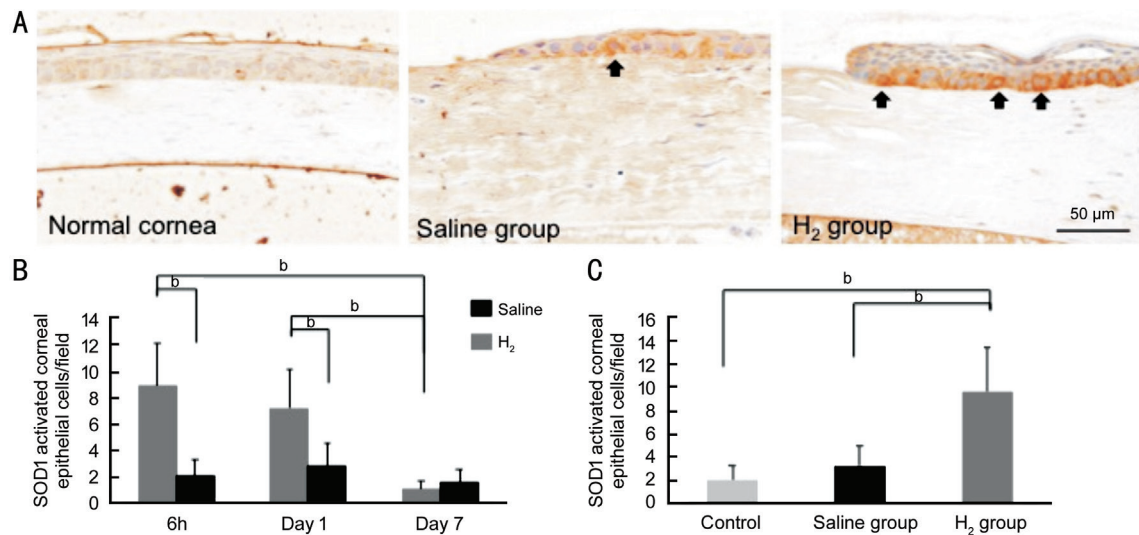


Figure 6 Increased cytoplasmic SOD1 expression in response to H₂ treatment A: Representative images of SOD1 (arrow) -immunostained corneal epithelial cells during wound healing after alkali injury; B: Bar chart demonstrating the activation of SOD1 in response to H₂ administration over time; C: Bar chart demonstrating that cytoplasmic SOD1 expression in the central cornea was significantly upregulated in the H₂ group vs the saline group and normal corneas at 6h post-injury. $n=30/104$ in total, $n=5$ for each group/for each endpoint. ^b $P<0.01$.

the anti-angiogenic effects of H₂ in the cornea. In our current study, our observation of the anti-angiogenic effect of H₂ agrees with the reported findings by Kubota *et al*^[6]. In our experiments, immunohistochemical staining for JG12 revealed the significant suppression of neovascularization in the H₂ group.

We additionally conducted a detailed analysis of the inflammatory cells infiltrating the injured corneal tissues. Immunohistochemical staining revealed a significantly smaller number of infiltrating neutrophils in the H₂ group relative to the saline group at all time points after injury. We further observed an association between infiltrating neutrophils and 8-OHdG-positive cells and observed that H₂ significantly suppressed both populations. As H₂ acts as a free radical scavenger, our findings indicate that a reduction in oxidative stress might help to suppress the inflammatory cell invasion, consistent with a previous report^[6]. We further confirmed this effect *via* observing corneal collagen using LV-SEM, a modality widely used to evaluate three-dimensional ultrastructural changes in tissues specimens intended for light microscopy^[19,25-26]. H₂ helped to maintain the normal alignment of stromal collagen fibers, an important factor in corneal transparency^[27].

We also observed a significant effect of H₂ on macrophage infiltration. Specifically, treatment with H₂ significantly reduced the infiltration of ED1-positive pan-macrophages while significantly increasing the infiltration of ED2-positive M2 macrophages. Notably, M1 macrophages are inflammatory cells, whereas M2 macrophage resolve inflammation and thus play critical roles in tissue remodeling and wound healing. Previous reports of corneal studies indicate that M2 macrophages function in the wound repair process in this tissue^[21,28]. Therefore, our observation that H₂ treatment

promotes M2 macrophage expression suggests another potential clinical application of this therapy. However, further experiments are needed to elucidate the pathological mechanism underlying the M1/M2 balance.

SODs are well-known players in antioxidant stress pathways. Of these enzymes, SOD1 is expressed in most tissues and is responsible for 90% of SOD activity^[13]. In SOD1-deficient animals, free radical-induced injuries lead to degenerative or inflammatory diseases^[29-30], and the observation of enhanced corneal alkali burn injury suggested the importance of SOD1 as an anti-free radical effector^[6]. In contrast, the use of instillation to abundantly increase the level of exogenous SOD1 in the eye appeared to reduce inflammation by resolving oxidative stress^[31]. Murakami *et al*^[32] have reported that treatment with H₂ indirectly reduces oxidative stress by inducing SOD through Nrf2 pathway. In the present study, therefore, we hypothesized that SOD1 might be involved in mechanism by which H₂ indirectly suppresses free radicals. Consistent with this hypothesis, we observed cytoplasmic SOD1 activation in response to H₂ in corneal epithelial cells even in the early stages of wound healing. Taken together, these results suggest that the anti-oxidative effects of H₂ involve not only a direct free radical scavenging effect, but also the activation of SOD1, consistent with a previous neurological study wherein H₂ was recognized as an effective treatment candidate for amyotrophic lateral sclerosis involving a mutation of cytosolic SOD1^[33].

In summary, our study of alkali-induced corneal injury revealed that H₂ exerts its anti-inflammatory effects not only by suppressing free radicals, but also by inducing the activation of SOD1. Further understanding of these characteristic effects of H₂ may enable additional ophthalmologic treatment strategies.

ACKNOWLEDGEMENTS

Conflicts of Interest: Arima T, None; Igarashi T, None; Uchiyama M, None; Kobayashi M, None; Ohsawa I, None; Shimizu A, None; Takahashi H, None.

REFERENCES

- Ohsawa I, Ishikawa M, Takahashi K, Watanabe M, Nishimaki K, Yamagata K, Katsura K, Katayama Y, Asoh S, Ohta S. Hydrogen acts as a therapeutic antioxidant by selectively reducing cytotoxic oxygen radicals. *Nat Med* 2007;13(6):688-694.
- Ohta S. Molecular hydrogen as a preventive and therapeutic medical gas: initiation, development and potential of hydrogen medicine. *Pharmacol Ther* 2014;144(1):1-11.
- Ichihara M, Sobue S, Ito M, Ito M, Hirayama M, Ohno K. Beneficial biological effects and the underlying mechanisms of molecular hydrogen - comprehensive review of 321 original articles. *Med Gas Res* 2015;5:12.
- Iketani M, Ohsawa I. Molecular hydrogen as a neuroprotective agent. *Curr Neuropharmacol* 2017;15(2):324-331.
- Oharazawa H, Igarashi T, Yokota T, Fujii H, Suzuki H, Machide M, Takahashi H, Ohta S, Ohsawa I. Protection of the retina by rapid diffusion of hydrogen: administration of hydrogen-loaded eye drops in retinal ischemia-reperfusion injury. *Invest Ophthalmol Vis Sci* 2010;51(1):487-492.
- Kubota M, Shimmura S, Kubota S, Miyashita H, Kato N, Noda K, Ozawa Y, Usui T, Ishida S, Umezawa K, Kurihara T, Tsubota K. Hydrogen and N-acetyl-L-cysteine rescue oxidative stress-induced angiogenesis in a mouse corneal alkali-burn model. *Invest Ophthalmol Vis Sci* 2011;52(1):427-433.
- Igarashi T, Ohsawa I, Kobayashi M, Igarashi T, Suzuki H, Iketani M, Takahashi H. Hydrogen prevents corneal endothelial damage in phacoemulsification cataract surgery. *Sci Rep* 2016;6:31190.
- Huang CS, Kawamura T, Toyoda Y, Nakao A. Recent advances in hydrogen research as a therapeutic medical gas. *Free Radic Res* 2010;44(9):971-982.
- Zhai X, Chen X, Shi JZ, Shi D, Ye ZH, Liu WW, Li M, Wang QJ, Kang ZM, Bi HD, Sun XJ. Lactulose ameliorates cerebral ischemia-reperfusion injury in rats by inducing hydrogen by activating Nrf2 expression. *Free Radic Biol Med* 2013;65:731-741.
- Park DJ, Agarwal A, George JF. Heme oxygenase-1 expression in murine dendritic cell subpopulations: effect on CD8+ dendritic cell differentiation *in vivo*. *Am J Pathol* 2010;176(6):2831-2839.
- Cai WW, Zhang MH, Yu YS, Cai JH. Treatment with hydrogen molecule alleviates TNF α -induced cell injury in osteoblast. *Mol Cell Biochem* 2013;373(1-2):1-9.
- Zhang YF, Sun Q, He B, Xiao J, Wang ZN, Sun XJ. Anti-inflammatory effect of hydrogen-rich saline in a rat model of regional myocardial ischemia and reperfusion. *Int J Cardiol* 2011;148(1):91-95.
- Crapo JD, Oury T, Rabouille C, Slot JW, Chang LY. Copper, zinc superoxide dismutase is primarily a cytosolic protein in human cells. *Proc Natl Acad Sci U S A* 1992;89(21):10405-10409.
- Masuda Y, Shimizu A, Mori T, Ishiwata T, Kitamura H, Ohashi R, Ishizaki M, Asano G, Sugisaki Y, Yamanaka N. Vascular endothelial growth factor enhances glomerular capillary repair and accelerates resolution of experimentally induced glomerulonephritis. *Am J Pathol* 2001;159(2):599-608.
- Inaga S, Kato M, Hirashima S, Munemura C, Okada S, Kameie T, Katsumoto T, Nakane H, Tanaka K, Hayashi K, Naguro T. Rapid three-dimensional analysis of renal biopsy sections by low vacuum scanning electron microscopy. *Arch Histol Cytol* 2011;73(3):113-125.
- Inaga S, Katsumoto T, Tanaka K, Kameie T, Nakane H, Naguro T. Platinum blue as an alternative to uranyl acetate for staining in transmission electron microscopy. *Arch Histol Cytol* 2007;70(1):43-49.
- Matsui K, Nagy-Bojarsky K, Laakkonen P, Krieger S, Mechtler K, Uchida S, Geleff S, Kang DH, Johnson RJ, Kerjaschki D, Kang DH. Lymphatic microvessels in the rat remnant kidney model of renal fibrosis: aminopeptidase P and podoplanin are discriminatory markers for endothelial cells of blood and lymphatic vessels. *J Am Soc Nephrol* 2003;14(8):1981-1989.
- Toyokuni S, Tanaka T, Hattori Y, Nishiyama Y, Yoshida A, Uchida K, Hiai H, Ochi H, Osawa T. Quantitative immunohistochemical determination of 8-hydroxy-2'-deoxyguanosine by a monoclonal antibody N45.1: its application to ferric nitrilotriacetate-induced renal carcinogenesis model. *Lab Invest* 1997;76(3):365-374.
- Inaga S, Hirashima S, Tanaka K, Katsumoto T, Kameie T, Nakane H, Naguro T. Low vacuum scanning electron microscopy for paraffin sections utilizing the differential stainability of cells and tissues with platinum blue. *Arch Histol Cytol* 2009;72(2):101-106.
- Arima T, Uchiyama M, Nakano Y, Nagasaka S, Kang DD, Shimizu A, Takahashi H. Peroxisome proliferator-activated receptor alpha agonist suppresses neovascularization by reducing both vascular endothelial growth factor and angiopoietin-2 in corneal alkali burn. *Sci Rep* 2017;7(1):17763.
- Saika S, Miyamoto T, Yamanaka O, Kato T, Ohnishi Y, Flanders KC, Ikeda K, Nakajima Y, Kao WW, Sato M, Muragaki Y, Ooshima A. Therapeutic effect of topical administration of SN50, an inhibitor of nuclear factor-kappaB, in treatment of corneal alkali burns in mice. *Am J Pathol* 2005;166(5):1393-1403.
- Nakano Y, Uchiyama M, Arima T, Nagasaka S, Igarashi T, Shimizu A, Takahashi H. PPAR α agonist suppresses inflammation after corneal alkali burn by suppressing proinflammatory cytokines, MCP-1, and nuclear translocation of NF- κ B. *Molecules* 2018;24(1):114.
- Feng M, Wang XH, Yang XB, Xiao Q, Jiang FG. Protective effect of saturated hydrogen saline against blue light-induced retinal damage in rats. *Int J Ophthalmol* 2012;5(2):151-157.
- Liu GD, Zhang H, Wang L, Han Q, Zhou SF, Liu P. Molecular hydrogen regulates the expression of miR-9, miR-21 and miR-199 in LPS-activated retinal microglia cells. *Int J Ophthalmol* 2013;6(3):280-285.
- Miyazaki H, Uozaki H, Tojo A, Hirashima S, Inaga S, Sakuma K, Morishita Y, Fukayama M. Application of low-vacuum scanning

- electron microscopy for renal biopsy specimens. *Pathol Res Pract* 2012;208(9):503-509.
- 26 Sawaguchi A, Kamimura T, Yamashita A, Takahashi N, Ichikawa K, Aoyama F, Asada Y. Informative three-dimensional survey of cell/tissue architectures in thick paraffin sections by simple low-vacuum scanning electron microscopy. *Sci Rep* 2018;8(1):7479.
- 27 Meek KM, Knupp C. Corneal structure and transparency. *Prog Retin Eye Res* 2015;49:1-16.
- 28 Oh JY, Lee HJ, Ko AY, Ko JH, Kim MK, Wee WR. Analysis of macrophage phenotype in rejected corneal allografts. *Invest Ophthalmol Vis Sci* 2013;54(12):7779-7784.
- 29 Imamura Y, Noda S, Hashizume K, Shinoda K, Yamaguchi M, Uchiyama S, Shimizu T, Mizushima Y, Shirasawa T, Tsubota K. Drusen, choroidal neovascularization, and retinal pigment epithelium dysfunction in SOD1-deficient mice: a model of age-related macular degeneration. *Proc Natl Acad Sci U S A* 2006;103(30):11282-11287.
- 30 Kojima T, Wakamatsu TH, Dogru M, Ogawa Y, Igarashi A, Ibrahim OM, Inaba T, Shimizu T, Noda S, Obata H, Nakamura S, Wakamatsu A, Shirasawa T, Shimazaki J, Negishi K, Tsubota K. Age-related dysfunction of the lacrimal gland and oxidative stress: evidence from the Cu, Zn-superoxide dismutase-1 (SOD1) knockout mice. *Am J Pathol* 2012;180(5):1879-1896.
- 31 Kost OA, Beznos OV, Davydova NG, Manickam DS, Nikolskaya II, Guller AE, Binevski PV, Chesnokova NB, Shekhter AB, Klyachko NL, Kabanov AV. Superoxide dismutase 1 nanozyme for treatment of eye inflammation. *Oxid Med Cell Longev* 2015;2015:5194239.
- 32 Murakami Y, Ito M, Ohsawa I. Molecular hydrogen protects against oxidative stress-induced SH-SY5Y neuroblastoma cell death through the process of mitohormesis. *PLoS One* 2017;12(5):e0176992.
- 33 Zhang Y, Li H, Yang C, Fan DF, Guo DZ, Hu HJ, Meng XG, Pan SY. Treatment with hydrogen-rich saline delays disease progression in a mouse model of amyotrophic lateral sclerosis. *Neurochem Res* 2016;41(4):770-778.